Space Sci Rev
DOI 10.1007/s11214-012-9884-2

Energy Spectra, Composition, and Other Properties of Ground-Level Events During Solar Cycle 23

R.A. Mewaldt · M.D. Looper · C.M.S. Cohen · D.K. Haggerty · A.W. Labrador · R.A. Leske · G.M. Mason · J.E. Mazur · T.T. von Rosenvinge

Received: 14 February 2011 / Accepted: 18 April 2012

Abstract We report spacecraft measurements of the energy spectra of solar protons and other solar energetic particle properties during the 16 Ground Level Events (GLEs) of Solar Cycle 23. The measurements were made by eight instruments on the ACE, GOES, SAMPEX, and STEREO spacecraft and extend from ∼0.1 to ∼500–700 MeV. All of the proton spectra exhibit spectral breaks at energies ranging from ∼2 to ∼46 MeV and all are well fit by a double power-law shape. A comparison of GLE events with a larger sample of other solar energetic particle (SEP) events shows that the typical spectral indices are harder in GLE events, with a mean slope of −3.18 at >40 MeV/nuc. In the energy range 45 to 80 MeV/nucleon about ∼50 % of GLE events have properties in common with impulsive ^{3}He-rich SEP events, including enrichments in Ne/O, Fe/O, ^{22}Ne/^{20}Ne, and elevated mean charge states of Fe. These ^{3}He-rich events contribute to the seed population accelerated by CME-driven shocks. An analysis is presented of whether highly-ionized Fe ions observed in five events could be due to electron stripping during shock acceleration in the low corona. Making use of stripping calculations by others and a coronal density model, we can account for events with mean Fe charge states of $\langle Q_{\mathrm{Fe}} \rangle \approx +20$ if the acceleration starts at ∼1.24–1.6 solar radii, consistent with recent comparisons of CME trajectories and type-II radio bursts. In addition, we suggest that gradual stripping of remnant ions from earlier large SEP events may also contribute a highly-ionized suprathermal seed population. We also discuss how

R.A. Mewaldt (✉) · C.M.S. Cohen · A.W. Labrador · R.A. Leske
Caltech, Pasadena, CA 91125, USA
e-mail: rmewaldt@srl.caltech.edu

M.D. Looper
The Aerospace Corporation, Los Angeles, CA 90009, USA

D.K. Haggerty · G.M. Mason
Johns Hopkins University/Applied Physics Laboratory, Laurel, MD 20723, USA

J.E. Mazur
The Aerospace Corporation, Chantilly, VA 20151, USA

T.T. von Rosenvinge
NASA/Goddard Space Flight Center, Greenbelt, MD 20771, USA

Published online: 30 May 2012

observed SEP spectral slopes relate to the energetics of particle acceleration in GLE and other large SEP events.

Keywords Sun: particle emission · Sun: coronal mass ejections (CMEs) · Acceleration of particles · Solar energetic particle acceleration · Sun: composition · Ionic charge states

1 Introduction

Ground-level events (GLEs) are large Solar Energetic Particle (SEP) events in which the intensity of high-energy solar protons is sufficient to rise above the galactic cosmic ray (GCR) background in one or more ground-based neutron monitors (e.g., Lopate 2006), muon detectors (Falcone et al. 2003; Abbasi et al. 2008), or ionization chambers (Forbush 1946). For high-latitude neutron monitors, the threshold for H (or He) is set by the thickness of the atmosphere at ∼500 MeV/nuc. GLEs are of space weather interest because they can present a risk to humans and hardware in space, as well as airline communications (Shea and Smart 2012). GLEs are of interest scientifically because they represent examples of events in which the particle acceleration process has apparently been more efficient, lasted longer, or been more widespread than in ∼90 % of more typical SEP events. During solar cycle 23 there were 16 GLEs, giving a total of 70 observed over the past ∼70 years. For all cycle 23 events there are direct measurements of proton energy spectra by spacecraft that extend from ∼0.1 MeV to 500–700 MeV. These 16 events were the subject of two interdisciplinary LWS workshops held in Palo Alto, CA in January 2009 and in Huntsville, AL in November 2009.

There have been a number of previously reported spacecraft measurements of GLE events over the energy range from ∼1 to several hundred MeV, in some cases compared to energy spectra derived from neutron monitor data (see, e.g., Lockwood et al. 1974; Debrunner et al. 1984, 1988; McGuire and von Rosenvinge 1984; Van Hollebeke et al. 1990). These authors favored energy spectra that included both power-laws and exponentials in either kinetic energy or rigidity, as well as Bessel functions in momentum/nuc. In this study we investigated fitting cycle-23 energy spectra with three separate spectral forms.

Previous studies have also reported that GLE events are very often enriched in heavy elements such as Fe. For example, Tylka et al. (2005) found that 23 of 25 GLE events from solar cycles 21 and 22 had Fe/O ratios that were elevated by at least a factor of 2 with respect to average SEP abundances (Reames 1995). We update these comparisons with new data from solar cycle 23, and also examine other related composition ratios. In particular, we examine the possibility that the presence of highly-ionized Fe in some of these events could be due to electron stripping in the low corona during or prior to the acceleration process.

In this paper we summarize spacecraft measurements of proton energy spectra, of the composition of abundant elements, and of other properties of the solar energetic particles (SEPs) observed *in situ* in the GLE events of solar cycle 23. We also discuss the energetics of large SEP events.

2 Observations

The spacecraft measurements reported here extend in energy from ∼100 keV/nuc to ∼500–700 MeV/nuc for protons and from 12 MeV/nuc to ∼80 MeV/nuc for heavier ions. They were made with instruments on NASA's ACE, SAMPEX, and STEREO missions and on

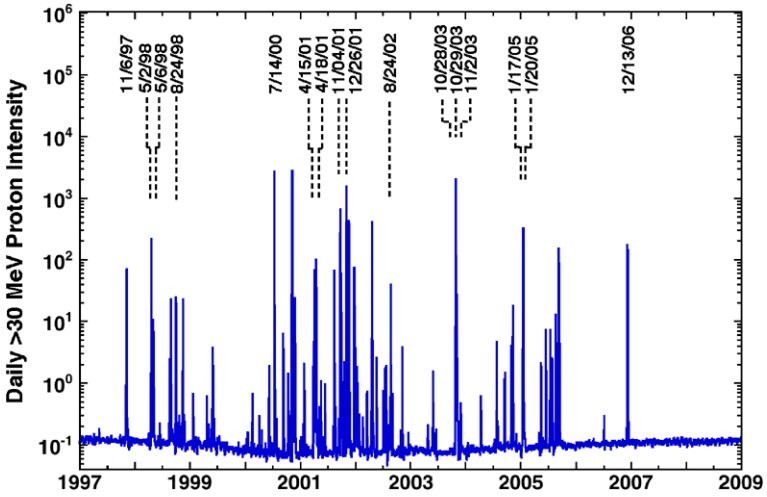

Fig. 1 Daily average intensities of >30 MeV protons in units of protons/cm^2 s from 1997 through 2008 as measured by the EPS instruments on GOES-8, GOES-11 and GOES-12. The dates of GLE events are labeled. In many cases these events are only days apart

NOAA's GOES-8, 10, 11, and 12 missions. ACE orbits the inner LaGrangian point (L1) providing continuous coverage of solar wind and SEP events that affect Earth. This paper includes proton data from the Electron, Proton, and Alpha Monitor (EPAM; Gold et al. 1998) and the Ultra-Low Energy Isotope Spectrometer (ULEIS; Mason et al. 1998), and composition data from the Solar Isotope Spectrometer (SIS; Stone et al. 1998).

SAMPEX is in a ∼600 km, 82° inclination orbit that provides two ∼15 minute high-latitude passes (>70° invariant latitude) during each ∼90 minute orbit (Baker et al. 1993). During polar passes the SAMPEX instruments are oriented towards the zenith. SAMPEX data from the Proton-Electron Telescope (PET; see Cook et al. 1993a and Mewaldt et al. 2005a) and the Mass Spectrometer Telescope (MAST; Cook et al. 1993b) are available for all but two of the 16 GLEs; during the May 1998 events SAMPEX was in a spin mode such that the telescopes were not always zenith-pointing at high latitudes. STEREO was launched in October 2006, just in time to record the last GLE of solar cycle 23. The SEP data included here are from the Low Energy Telescope (Mewaldt et al. 2008a) and the High Energy Telescope (von Rosenvinge et al. 2008). The twin STEREO spacecraft are separating from Earth at ∼22.5° per year.

NOAA's GOES satellites are in geosynchronous orbit at $L = 6.6$ where geomagnetic effects are relatively minor for protons >10 MeV. Data reported here are from the EPS and HEPAD sensors (Onsager et al. 1996). Use of GOES proton spectra from ∼10 to ∼200 MeV is described in Mewaldt et al. (2005a). The HEPAD spectra from 350 to 700 MeV have been corrected as described in Smart and Shea (1999). All spectra and composition measurements have been corrected for contributions due to anomalous cosmic rays and galactic cosmic rays (GCRs).

The time history of >30 MeV proton intensities during solar cycle 23 is shown in Fig. 1. The sixteen ground-level events that occurred during this period are indicated. Although all of the GLEs were among the top 50 events, when ordered by >30 MeV fluence, there are a few events early in the cycle that do not stand out at >30 MeV (e.g., 6 November 1997 and 24 August 1998). On the other hand, the 8 November 2000 event (N10W75), which had the

third-largest >30 MeV fluence of cycle 23, was not detected as a GLE. These comparisons suggest that there are significant differences in the energy spectra and/or time histories of large SEP events.

We consider here three spectral forms for fitting GLE spectra. In a 1979 article Ramaty (1979) considered the stochastic Fermi acceleration of solar energetic particles in a turbulent, tenuous plasma carrying a magnetic field. He obtained an energy spectrum parameterized by the product αT, where α is an acceleration efficiency and T is the escape time from the acceleration region. The non-relativistic solution can be written in terms of a Bessel function in momentum per nucleon (p):

$$dJ/dE = ApK_2\big[(12/mc)(p/\alpha T)\big]^{1/2}. \tag{1}$$

Here J is intensity or fluence, E is kinetic energy/nucleon, A is a normalization constant, K_2 is the modified Bessel function of the 2nd kind, m is the proton mass, and c is the speed of light. Ramaty and co-workers used this form in a variety of applications (e.g., Forman et al. 1986; Ramaty and Murphy 1987). In 1984 McGuire and von Rosenvinge used this spectral form to fit proton and alpha time-of-maximum spectra from ~1 to >100 MeV/nuc for several large SEP events and concluded that overall, the Bessel function form fit better than an exponential in rigidity or a single power-law. They also provided an alternate form of this function derived by asymptotic expansion of the Bessel function:

$$dJ/dE = AE^{3/8}\exp\big[-\big(E/\big(3.26(\alpha T)^2\big)\big)^{1/4}\big]. \tag{2}$$

We also consider two additional spectral forms. Ellison and Ramaty (1985) proposed that solar particle spectra accelerated by shocks would have spectra of the form

$$dJ/dE = KE^{\gamma}\exp(-E/E_0) \tag{3}$$

where K, E_0, and γ are constants. This power-law shape with an exponential rollover was used by Mazur et al. (1992), Tylka et al. (2000), and Tylka (2001). Mewaldt et al. (2005a) fit H, He, and O fluence spectra with both the Ellison-Ramaty shape and with the double-power-law shape originally proposed by Band et al. (1993) for fitting γ-ray burst spectra. The equation for this latter spectral shape is given by:

$$\begin{aligned} dJ/dE &= CE^{\gamma_1}\exp(-E/E_0) \quad \text{for } E \le (\gamma_1-\gamma_2)E_0; \\ dJ/dE &= CE^{\gamma_2}\big\{\big[(\gamma_1-\gamma_2)E_0\big]^{(\gamma_1-\gamma_2)}\exp(\gamma_2-\gamma_1)\big\} \quad \text{for } E \ge (\gamma_1-\gamma_2)E_0, \end{aligned} \tag{4}$$

where γ_1 is the low-energy power-law slope and γ_2 is the high-energy power-law slope and E and E_0 are measured in energy/nucleon. The function is identical to the Ellison-Ramaty form below the transition energy, $(\gamma_1-\gamma_2)E_0$. There is a smooth transition to a second power law at higher energies. In a study of the five large "Halloween" SEP events Mewaldt et al. (2005a) concluded that the Band formulation fit best (see also Tylka et al. 2005, 2006). McGuire and von Rosenvinge (1984) also noted that their spectra could be fit by two power-laws, but favored the Bessel function form because it involved fewer free parameters. The SEP spectra measured by Van Hollebeke et al. (1990) in two Fe-rich γ-ray/neutron events (one of which was a GLE) also appear to have a double power-law shape.

In Fig. 2 (left panel) we compare three fits to the proton fluence spectrum for the 2 November 2003 GLE event. It is clear that only the Band function is able to reproduce the high-energy spectra above ~100 MeV. Figure 2 (right panel) shows fits to the 13 December 2006 event, which had a somewhat harder spectrum at high energy. In this case the best-fit Bessel function begins to fail at ~40 MeV and by ~400 MeV it falls more than a factor of 100 below the measured spectra. The Ellison-Ramaty fit for the 13 December 2006 event

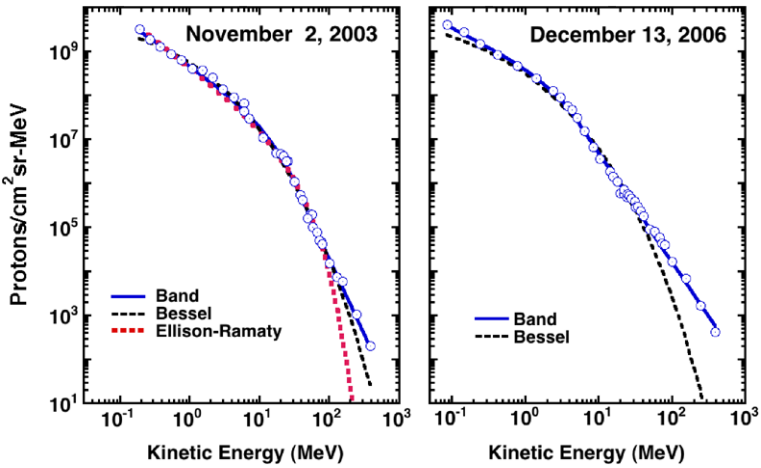

Fig. 2 (*Left*) Fluence spectra measured by ACE/ULEIS, SAMPEX/PET, and GOES-11 during the 2 November 2003 event are fit with the double power-law shape of Band et al. (1993); the power-law with exponential-tail shape of Ellison and Ramaty (1985), and the Bessel function shape of Ramaty (1979). (*Right*) The Band et al. and Bessel spectral shapes are fit to fluence spectra measured by ACE/EPAM, STEREO/LET, STEREO/HET, SAMPEX/PET, and GOES-11 during the 13 December 2006 SEP event. Note that only the Band et al. function can provide a reasonable fit up to the highest observed energies

(not shown), provided an even poorer overall fit, fitting the high energy points from ∼15 to 400 MeV with an e-folding energy of $E_0 \sim 110$ MeV, but failing entirely to fit the spectral break at several MeV.

Figures 3, 4, 5 and 6 show proton fluence spectra for the sixteen GLE events. For all sixteen events the spectra from ∼0.1 to ∼500–700 MeV were fit with the three spectral forms in Fig. 2. In all 16 cases the double power-law form of Band et al. (1993) had the lowest reduced-X^2 (on average ∼2 times lower than the Ellison-Ramaty form and ∼4 times lower than the Bessel function form). Fitting parameters for the Band et al. (1993) function are listed in Table 1. Having an accurate representation of the fluence of the largest SEP events is important for specifying the interplanetary radiation environment (Mewaldt et al. 2005b; Baker et al. 2006).

All sixteen spectra have breaks with "break energies" (defined by the intersection of the two power laws) that range from ∼2 to 46 MeV. In the fluence spectrum integrated over the entire 24 August 1998 event there is a hardening of the spectrum that can be seen in the red points above ∼100 MeV (lower right panel of Fig. 3). It was found that most of the >100 MeV contribution came during the first 20 hours of the event, during which the spectrum was harder at both low and high energies (see dashed line in the lower right panel of Fig. 3). In general, high-energy particles in large SEP events arrive and decay away earlier than those at lower energies because of their higher velocities and larger diffusion coefficients in the interplanetary magnetic field (see e.g., Li et al. 2003).

In measuring SEP fluence spectra at 1 AU some judgment is needed to decide when an SEP event started, and then either decayed to background, or was overtaken by a subsequent event. Fortunately, this is generally less of an issue for GLE events, which rise further above the background than most SEP events. The general procedure was to start with higher energy (>10 MeV/nuc) heavy-ion data from ACE/SIS and GOES proton data, where contributions from CIR events and other interplanetary sources are seldom an issue. Using hourly averages, the integration was started in the first hour following the solar eruption that a

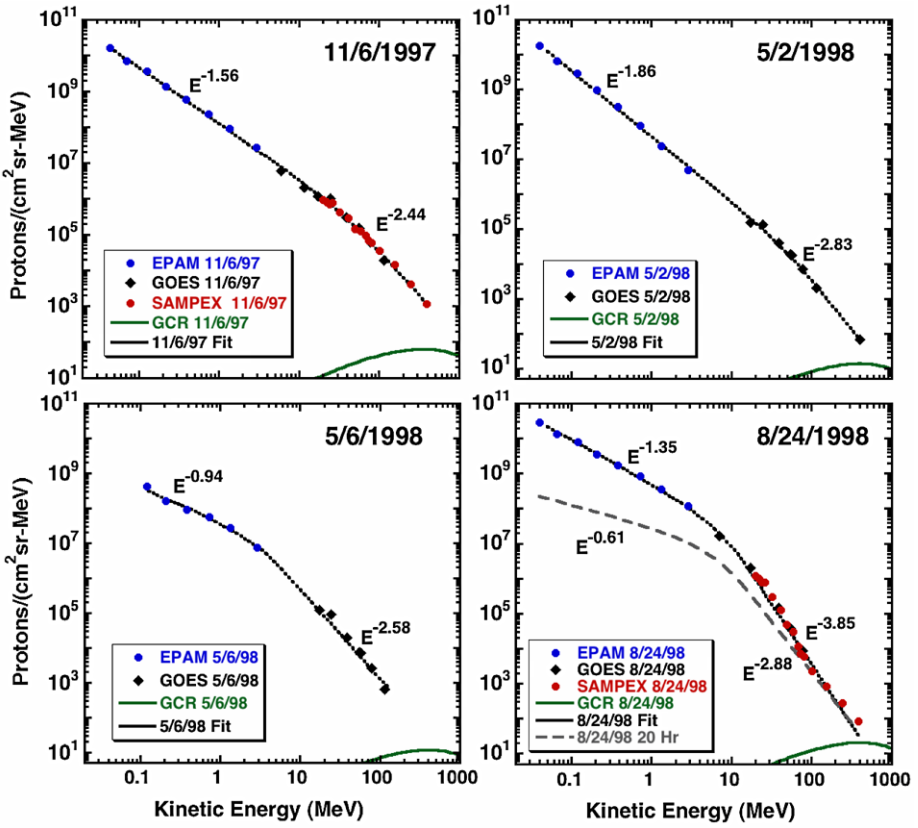

Fig. 3 Measured proton fluence spectra for the first four GLE events of solar cycle 23 are fit with the double power-law function of Band et al. (1993). The asymptotic spectral slopes above and below the break energy are indicated. Nominal GCR fluences are also shown for the time interval used for the highest energy points. The plotted points have been corrected for GCR contributions. Also shown for the August 24, 1998 event is the measured fluence during the first 20 hours, which has a harder spectrum and accounts for most of the high energy fluence

significant increase began and continued rising to a maximum. If a second event followed closely the fluence integration was terminated at the intensity minimum between the two events. These start and end times were also used for the SAMPEX data analysis, where the data were available from two polar passes per ∼90 minute orbit, using only data from invariant latitudes >70° (see Mewaldt et al. 2005a). For the >350 MeV HEPAD data, it was found that the SEP intensity often rose above background only during the first day or two, so these fluence integrations were often terminated earlier than at lower energies.

For the lower energy (<5 MeV) ULEIS and EPAM data the >10 MeV start and end times served as starting points, but count rates from the various energy intervals were examined to determine improved start and end times that took into account when low-energy particles started to rise above background and they were checked to assure that any related ESP contributions were included, without including new SEP or CIR events. In all cases, quiet-time pre-event background was subtracted from each hour to eliminate contributions from galactic cosmic rays, anomalous cosmic rays, and instrumental background (see also the discussion in Mewaldt et al. 2005a).

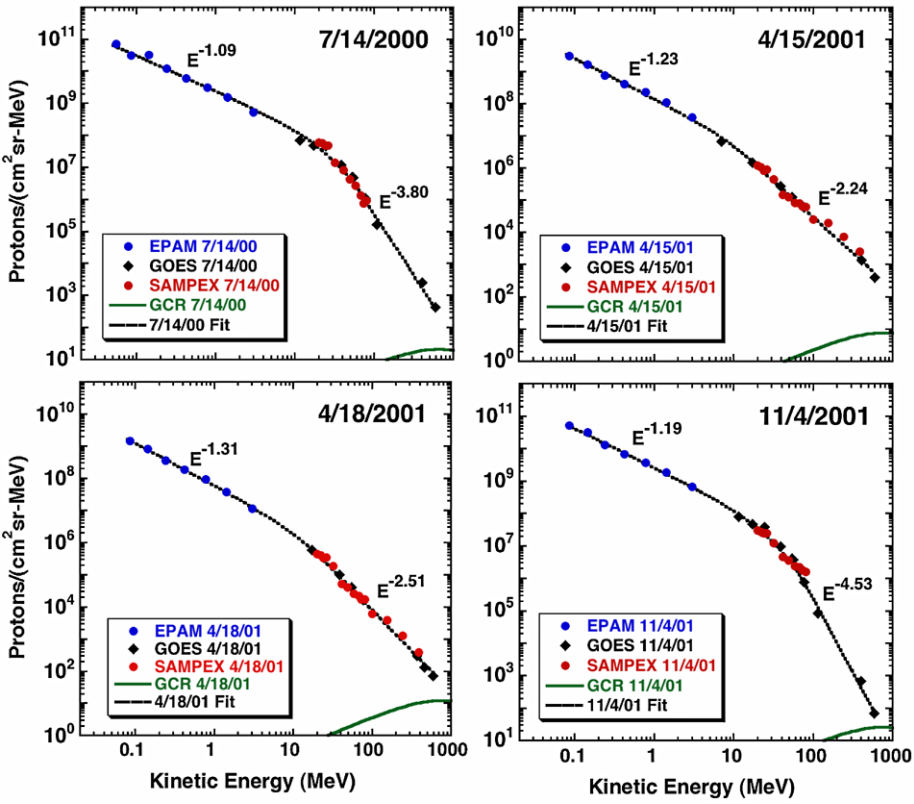

Fig. 4 Proton fluence spectra for GLE events 5–8 from solar cycle 23 (see also the caption for Fig. 3)

Tables listing the measured spectral points, the fitting parameters, the start and end times for the various energy intervals, and the composition data discussed below can be found at the ACE Science Center at the following location: http://www.srl.caltech.edu/ACE/ASC/DATA/level3/GLE/index.html.

In Fig. 7 the range of spectral indices above the break energy for the 16 GLE fits is compared with those for 22 large non-GLE events fit with the same function. On average, GLE energy spectra greater than ∼40 MeV are significantly harder than those of typical large SEP events. The spectral slopes below the break-energies are similar, with both samples having a mean slope of approximately −1.25.

A number of studies have compared spectra measured *in situ* with spacecraft instruments with spectra derived using the cutoff rigidities of various neutron monitors, including Lockwood et al. (1974), and Debrunner et al. (1984, 1988). From these studies it is clear that GLE spectra typically steepen further at energies >0.5 GeV.

Tylka and Dietrich (2009) have derived integral rigidity spectra for many GLE events based on the responses of neutron monitors with a wide range of geomagnetic cutoffs and also using GOES data. They find that the integral rigidity spectra of GLE events are well-fit by the function of Band et al. (1993). Like earlier studies they find that the spectra typically steepen at rigidities greater than ∼1 GV (∼440 MeV), with average integral spectral slopes in rigidity of −5 to −7. Cross checks with the spectra reported here (which start at much lower energy) show good agreement in the region of overlap (Tylka 2009).

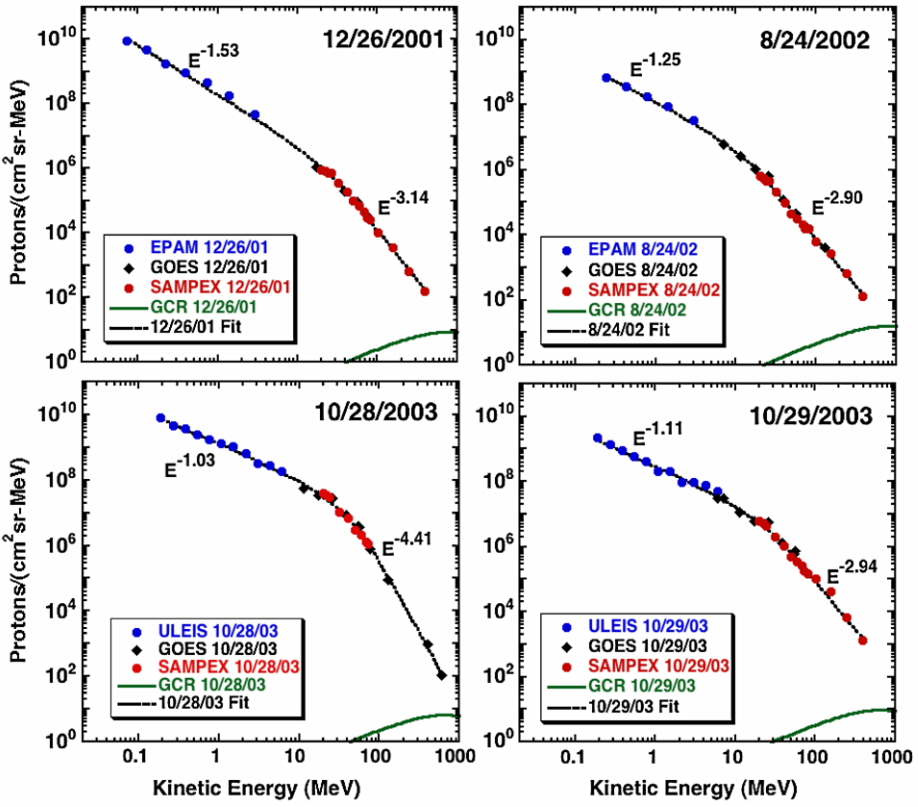

Fig. 5 Proton fluence spectra for GLE events 9–12 from solar cycle 23 (see also the caption for Fig. 3)

3 Other Properties of Ground Level SEP Events

In this section we compare in situ measurements of several properties of GLE events with those of other large (non-GLE) SEP events. Some of these properties are summarized in Table 2.

The Fe/O ratio is often used to characterize SEP events and has been considered to be a diagnostic of the presence of flare material (e.g., Reames et al. 1994; Cane et al. 2003, 2006) because it is elevated in (much smaller) ^{3}He-rich flare-related events (e.g., Mason et al. 1994; Leske et al. 2007). In Fig. 8 the >30 MeV proton fluence is plotted versus the Fe/O ratio at 45–80 MeV/nuc for the 16 cycle-23 GLE events and for a sample of 30 non-GLE events with >30 MeV proton fluences $> 3 \times 10^6$ per cm^2. Note that Fe/O varies by a factor of ~100 or more in the GLE and non-GLE samples. These two samples of SEP events also have a similar distribution of >30 MeV proton fluences. Overall, during solar cycle 23 GLE events were more likely to be enriched by at least ×2 in Fe (56 ± 12 % of the 16 events) than were non-GLE events of similar intensities (33 ± 8 % of the events).

Some non-GLE events in the right panel of Fig. 8 have ~50–500 times the >30 MeV proton fluence of some GLE events in the left panel, yet they fail to result in GLE events (an example is the 8 November 2000 event, which had the third largest >30 MeV proton fluence of solar cycle 23; see Fig. 1). Such "failed" GLE events are presumably due in large part to spectral differences (see Fig. 7 and Sect. 4) as well as to the much more gradual time

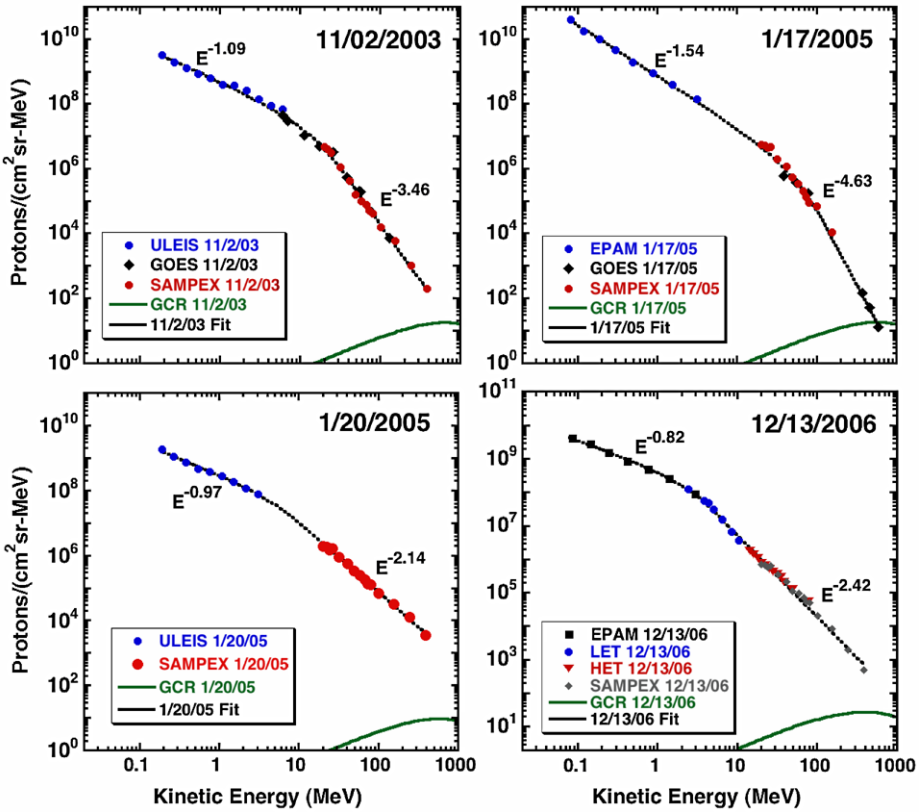

Fig. 6 Proton fluence spectra for GLE events 13–16 from solar cycle 23 (see also the caption for Fig. 3)

Table 1 GLE double power-law fitting parameters

Event	Normalization	γ_1	γ_2	E_0
11/6/97	1.28 ± 0.07 E+08	-1.56 ± 0.03	-2.44 ± 0.14	91.3 ± 18.8
5/2/98	4.49 ± 0.30 E+07	-1.86 ± 0.02	-2.83 ± 0.20	$114. \pm 32.$
5/6/98	4.59 ± 0.86 E+07	-0.94 ± 0.14	-2.58 ± 0.08	3.81 ± 1.16
8/24/98	5.27 ± 0.49 E+08	-1.35 ± 0.05	-3.85 ± 0.11	10.6 ± 1.17
7/14/00	2.48 ± 0.15 E+09	-1.09 ± 0.03	-3.80 ± 0.10	24.2 ± 1.9
4/15/01	1.51 ± 0.16 E+08	-1.23 ± 0.07	-2.24 ± 0.04	16.1 ± 4.7
4/18/01	6.05 ± 0.62 E+07	-1.31 ± 0.07	-2.51 ± 0.05	19.9 ± 5.1
11/4/01	2.68 ± 0.17 E+09	-1.19 ± 0.03	-4.53 ± 0.11	25.4 ± 1.8
12/26/01	1.94 ± 0.16 E+08	-1.53 ± 0.04	-3.14 ± 0.13	31.7 ± 5.5
8/24/02	1.28 ± 0.12 E+08	-1.25 ± 0.08	-2.90 ± 0.06	14.5 ± 2.8
10/28/03	1.37 ± 0.08 E+09	-1.03 ± 0.04	-4.41 ± 0.12	27.0 ± 2.1
10/29/03	3.03 ± 0.17 E+08	-1.11 ± 0.05	-2.94 ± 0.13	27.7 ± 3.4
11/2/03	4.94 ± 0.31 E+08	-1.09 ± 0.05	-3.46 ± 0.12	13.3 ± 1.5
1/17/05	7.37 ± 0.48 E+08	-1.54 ± 0.04	-4.63 ± 0.15	40.5 ± 4.4
1/20/05	3.22 ± 0.34 E+08	-0.97 ± 0.11	-2.14 ± 0.06	8.18 ± 2.63
12/13/06	5.25 ± 0.85 E+08	-0.82 ± 0.10	-2.42 ± 0.03	3.01 ± 0.66

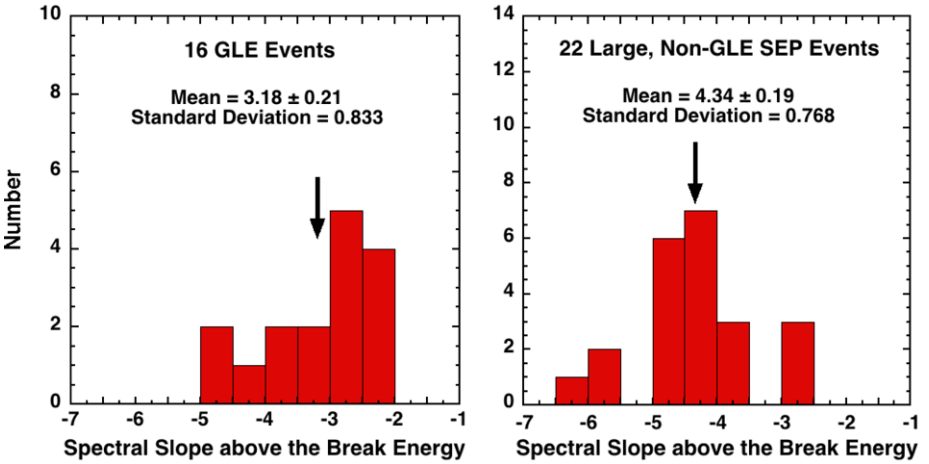

Fig. 7 (*Left*): Histograms of the spectral index above the spectral break (γ_2 in Table 1) for the 16 GLE events of cycle 23 and (*right*) for 22 non-GLE events from cycle 23. Note that, on average, GLE events have significantly harder spectra at high energies

Table 2 Selected properties of GLE events

Date	X-ray intensity	Location[1]	>30 MeV proton fluence[2]	Ne/O 12–45 MeV/n	Fe/O 12–45 MeV/n	Fe/O 45–80 MeV/n
11/6/97	X9.4	S18W63	1.63 e+08	0.284 ± 0.003	0.733 ± 0.007	0.765 ± 0.018
5/2/98	X1.1	S15W15	1.85 e+07	0.342 ± 0.010	0.683 ± 0.016	0.674 ± 0.058
5/6/98	X2.7	S11W65	8.02 e+06	0.324 ± 0.010	0.531 ± 0.014	0.294 ± 0.068
8/24/98	X1.0	N35E09	4.69 e+07	0.176 ± 0.002	0.018 ± 0.001	0.863 ± 0.165
7/14/00	X5.7	N22W07	4.31 e+09	0.167 ± 0.003	0.099 ± 0.010	0.106 ± 0.005
4/15/01	X14	S20W85	1.45 e+08	0.186 ± 0.004	0.486 ± 0.010	0.813 ± 0.043
4/18/01	?	S23W117	4.48 e+07	0.173 ± 0.004	0.186 ± 0.004	0.519 ± 0.049
11/4/01	X1.0	N06W18	3.40 e+09	0.135 ± 0.004	0.067 ± 0.007	0.038 ± 0.002
12/26/01	M7.1	N08W54	1.16 e+07	0.137 ± 0.002	0.412 ± 0.008	0.671 ± 0.029
8/24/02	X3.1	S02W81	5.30 e+07	0.150 ± 0.003	0.222 ± 0.004	0.824 ± 0.076
10/28/03	X17	S20E02	3.07 e+09	0.114 ± 0.002	0.041 ± 0.004	0.0060 ± 0.0009
10/29/03	X10	S19W09	5.34 e+08	0.248 ± 0.002	0.141 ± 0.007	0.126 ± 0.008
11/2/03	X8.3	S18W59	1.95 e+08	0.135 ± 0.002	0.043 ± 0.001	0.118 ± 0.010
1/17/05	X3.8	N14W25	6.50 e+08	0.177 ± 0.002	0.031 ± 0.001	0.010 ± 0.001
1/20/05	X7.1	N14W61	4.10 e+08	0.246 ± 0.003	0.198 ± 0.010	0.188 ± 0.005
12/13/06	X3.4	S06W23	1.67 e+08	0.215 ± 0.002	0.778 ± 0.016	0.804 ± 0.020

[1] Flare locations from Cane et al. (2006)

[2] Units for the proton fluences (measured by GOES) are protons/cm^2

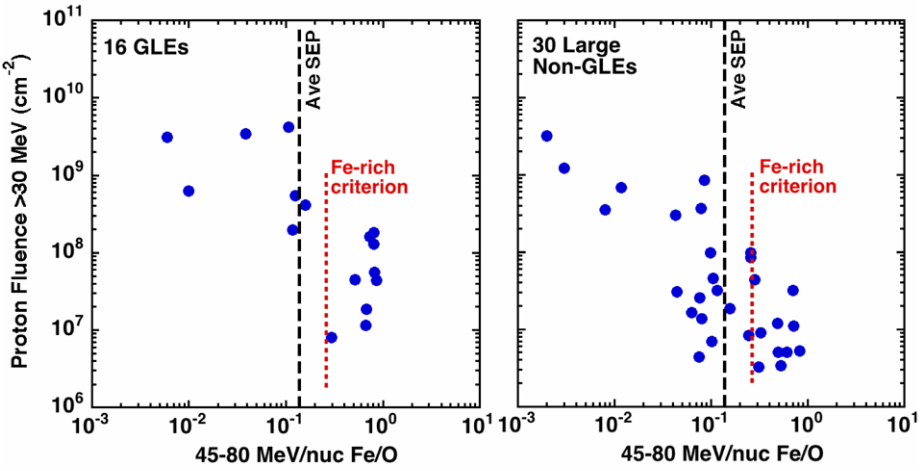

Fig. 8 The >30 MeV proton fluence from GOES/EPI is plotted versus the 45–80 MeV/nuc Fe/O ratio measured by ACE/SIS for the 16 GLE events of cycle 23 (*left*) and for 30 non-GLE events observed from 1997 through 2006 (*right*). The non-GLE events were required to have fluences of $>3 \times 10^6$ protons/cm^2 > 30 MeV and measurable Fe/O ratios in the 45–80 MeV/nuc energy range. Also indicated is the average 5–12 MeV/nuc ratio of Fe/O = 0.134 reported by Reames (1995) and the criterion for Fe-rich GLE events adopted by Tylka et al. (2005) for solar-cycle 21 and 22 events (Fe/O ≥ 0.268)

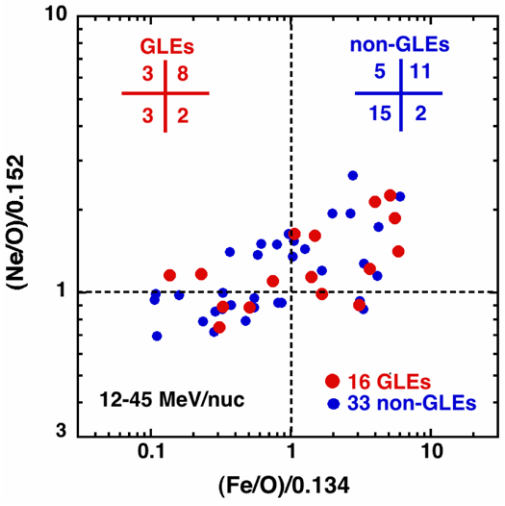

Fig. 9 The 12–45 MeV/nuc Ne/O ratio is plotted versus the 12–45 MeV/nuc Fe/O ratio for the 16 GLE events (*red*) and for 33 other SEP events. Both ratios are normalized to the average 5–12 MeV/nuc SEP abundance ratios from Reames (1995). Note the general correlation of Ne/O with Fe/O and that 8 of the 16 GLE events are in the upper right-hand quadrant of the plot. Adapted from Mewaldt et al. (2007)

profiles of eastern-hemisphere events, which may have large fluences, but never reach peak intensities that stand out above the >0.5 GeV GCR background. One noticeable feature is that the Fe-rich GLEs, on average, have 1–2 orders of magnitude smaller >30 MeV proton fluences than the Fe-poor GLEs (Tylka et al. 2005; Mewaldt et al. 2006).

Another element abundance ratio that has been used as a signature of flare material is Ne/O (Reames et al. 1994; Mewaldt et al. 2007). Figure 9 illustrates that Fe/O and Ne/O are correlated for both GLE and non-GLE events. Compared to the average SEP abundances

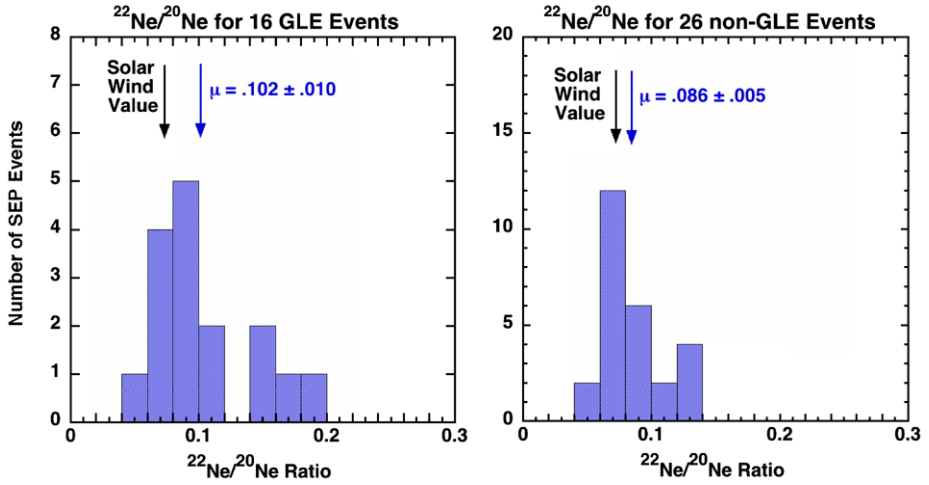

Fig. 10 The ^{22}Ne/^{20}Ne ratio in GLEs (*left panel*) is somewhat greater than in non-GLE events (*right panel*). The average solar wind value of 0.0716 ± 0.0001 (Meshik et al. 2007) is also shown. Enriched ^{22}Ne is one of several characteristics of impulsive flare material (Mason et al. 1994; Leske et al. 2007), but can also result from charge-to-mass (Q/M) dependent fractionation during acceleration and transport

at 5–12 MeV/nuc (Reames 1995), 10 of the 16 GLEs are Fe-rich and 10 are Ne-rich in the 12–45 MeV/nuc interval.

An enrichment in the ^{22}Ne/^{20}Ne ratio is also a possible signature of flare contributions, since small ^{3}He-rich events associated with reconnection jets typically have an elevated ^{22}Ne/^{20}Ne ratio with respect to that in the solar wind (Mason et al. 1994; Leske et al. 2007). As shown in Fig. 10, the mean ^{22}Ne/^{20}Ne ratio for GLE events is enriched by a factor of $\sim$1.4 with respect to the solar-wind ratio (^{22}Ne/^{20}Ne = 0.0716; Meshik et al. 2007), and enriched by $\sim$27 % relative to the mean of 26 non-GLE events.

A fourth possible signature of contributions from flare-accelerated material is the presence of material with highly-ionized charge-states, especially Fe. In solar wind the mean charge state of Fe is typically about +10, but in small impulsive flare events Klecker et al. (2007) find that the mean charge state ranges from $\sim$ +14 to +18 from $\sim$0.08 to $\sim$0.5 MeV/nuc (see also Klecker et al. 2006). For energies >20 MeV/nuc mean ionic charge states can be measured using the geomagnetic technique (Leske et al. 1995; Labrador et al. 2005).

In Fig. 11 we compare the mean charge state of Fe, $\langle Q_{\mathrm{Fe}} \rangle$, for ten GLE events and nine non-GLE events. Included are SAMPEX/MAST measurements using the geomagnetic technique (see Labrador et al. 2005) and three values obtained by indirect approaches based on fitting the composition and spectra of heavy ions (Cohen et al. 1999a, 1999b; Tylka et al. 2000). For other examples of indirect SEP charge state estimates see Dietrich and Lopate (1999) and Sollitt et al. (2008). While the range of mean charge states for SEP Fe is similar to that in non-GLEs, the mean value of $\langle Q_{\mathrm{Fe}} \rangle$ for the GLEs is somewhat greater (by $\sim 1.1\,\sigma$) than that for non-GLE events. Possible origins of elevated charge states are discussed below. Enrichments in Fe/O, Ne/O, ^{22}Ne/^{20}Ne, and high ionic-charge states generally occur in the same SEP events, including all four events in 1997–1998, the April and December events in 2001, and the December 2006 event (e.g., Cohen et al. 1999a, 1999b; Labrador et al. 2005; Mewaldt et al. 2006).

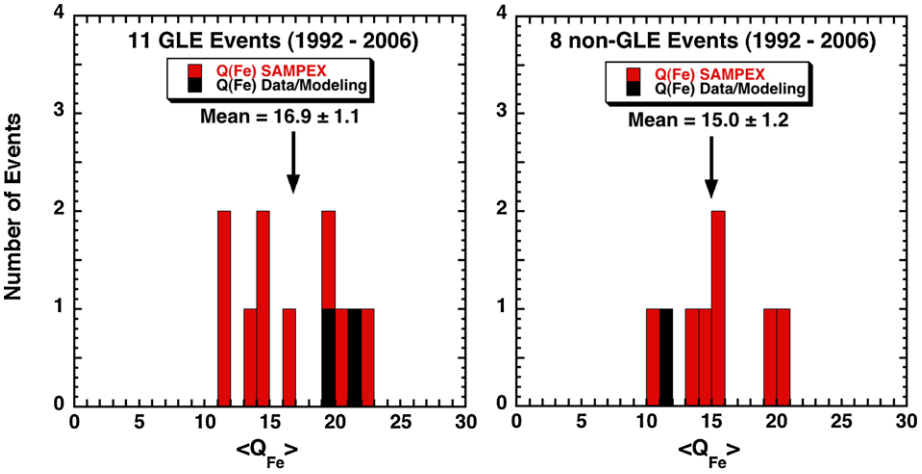

Fig. 11 The mean charge-state of Fe in GLEs is somewhat greater than in a sample of other large SEP events. The measurements are from SAMPEX/MAST in the energy interval from ∼25 to ∼80 MeV/nuc (Leske et al. 1995; Labrador et al. 2005; Mewaldt et al. 2006). Also shown (in black) are charge-state estimates obtained indirectly by fitting SEP abundance variations and time profiles using Q/M-dependent functions (Cohen et al. 1999a, 1999b; Tylka et al. 2000; Dietrich and Tylka 2003). These indirect estimates are included in the quoted means

4 Discussion

Energy Spectra In an earlier study of SEP proton and He spectra from ∼1 to ∼400 MeV/nuc McGuire and von Rosenvinge (1984) found that modified Bessel functions of the 2nd kind provided the best fit. However, their spectra were based on time-of-maximum intensities rather than fluences, and, more importantly, their measurements did not extend as low in energy as the spectra in Figs. 3–6. As a result they could not observe the power-law behavior that we observe below ∼1 MeV/nuc for all species (Figs. 3–6; see also Mewaldt et al. 2005a; Cohen et al. 2005). McGuire and von Rosenvinge also commented that two power laws might fit just as well, but would require additional free parameters. With the extension to lower energies provided in solar cycle 23 by the ULEIS and EPAM instruments on ACE, and the high-energy coverage provided by GOES and SAMPEX, the range of spectral forms that can fit fluence spectra of large SEP events from ∼0.05 to ∼500 MeV/nucleon is much more limited, and whenever there is adequate energy coverage at high energies (e.g., >200 MeV), the double power-law form of Band et al. (1993) generally fits best (see also Mewaldt et al. 2005a).

Tylka et al. (2000) showed that spectral roll-overs for different species were related to their charge to mass ratios (Q/A; see also Mewaldt et al. 2005b). Cohen et al. (2003, 2005) showed that the break energy for different elements could be organized by $(Q/A)^{\delta}$, with the breaks occurring at the same value of the diffusion coefficient (κ) and with δ varying from event to event. By equating κ for different heavy ions Cohen et al. (2003, 2005) were able to relate the breaks to turbulence power spectra, and suggested that proton-amplified Alfven waves might be the source of variations in the turbulence spectra during large SEP events (see also Mewaldt et al. 2005a).

Surprisingly, there have been relatively few attempts to explain why the spectral breaks result in double power-law spectra. In particular, it is important to understand what determines the spectral slope beyond the break. Vainio (2003) has shown that a double-power-law

spectrum can result from a single power-law accelerated spectrum that is subject to the effects of proton-amplified Alfven waves near the Sun. These waves trap low-energy protons near the shock below a typical breakpoint energy of ∼10 MeV, but allow higher energy particles to escape. Vainio obtained an E^{-1} power law below ∼10 MeV and a somewhat steeper $E^{-1.6}$ power law up to ∼100 MeV for the event he considered as an example. In a similar approach, Li et al. (2005; see also Li et al. 2009) produced a spectral break followed by a second power law by introducing a loss term in the transport equation to reflect the leakage of accelerated particles from the shocked upstream region. A broken power-law resulted if the diffusion coefficient had a step-like feature as a function of rigidity.

In the semi-empirical model of Tylka and Lee (2006), a quasi-perpendicular shock produces spectra that appear to be consistent with a double power-law (see their Fig. 4b). For the 16 events reported here, a significant fraction have characteristics that are consistent with the Tylka and Lee expectations for acceleration at quasi-perpendicular shocks, including hard spectra at high energies (γ_2 in Table 1 and Fig. 7), and, in particular, an elevated Fe/O ratio at high energies (Table 2). Examples include the 6 November 1997, 2 May 1998, 15 April 2001, 18 April 2001, 26 December 2001, 24 August 2002, and 13 December 2006 events. However, for quasi-parallel shocks the Tylka and Lee (2006) model predicts an exponential roll-over at high energies (see their Fig. 4b). All of the sixteen GLE events reported here had proton spectra that were better fit by a double power-law form than an exponential roll-over (see Sect. 2 and also Mewaldt et al. 2005a).

Reames and Ng (2010) have analyzed the effects of proton-amplified Alfven waves in seven of the 16 GLE events discussed here. In six of their seven events there is clear evidence that the time-intensity profiles are affected by the "streaming-limit", an equilibrium intensity that is established when outwardly-streaming protons amplify resonant Alfven waves that then scatter subsequent energetic protons, thereby reducing the streaming. The result is that for sufficiently intense (mainly near-central meridian) events the ion intensities at 1 AU at energies less than ∼40 MeV/nuc can reach a plateau (the streaming limit) that may last for ∼1 day. For plots of how the streaming limit affects the time history of several GLE events see Reames and Ng (2010).

Once the CME shock arrives at 1 AU, the ion intensity in the energetic storm particle (ESP) event can increase by 1–2 orders of magnitude for a period of up to ∼12 hours, including most of the low-energy ion fluence for the event. For example, in the 14 July 2000 Bastille Day event (which lasted more than 4 days), the fraction of the total proton fluence that occurred during the 12 hours surrounding the shock arrival ranged from ∼70 % at ∼1 MeV to ∼40 % at ∼40 MeV. For >100 MeV protons only ∼10–15 % of the fluence arrived during this interval. Similar numbers are obtained from the 28 October 2003 event (see also the 8/24/98 spectrum in Fig. 3, where most of the high energy particles arrived in the first 20 hours, but the lower energies were suppressed during this time). In the twelve cycle-23 GLE events with an ESP contribution the importance of the fluence contribution at 1 MeV ranged from minor to dominant.

By contrast, in the 6 May 1998 event, which did not have an ESP contribution, the first 12 hours of the event included ∼80 % of the 15 MeV to 200 MeV protons, and 30 % to 55 % of 1 to 6 MeV protons. Thus in many GLE events most of the low-energy fluence remains trapped near the shock until it arrives. This makes it difficult to relate observed energy spectra below the spectral break to shock acceleration theory without benefit of a very detailed model.

The comparisons presented here indicate that, on average, the 16 GLEs of solar cycle 23 differ in several ways from other large SEP events. The most significant difference is in the spectral index above the spectral break in the proton spectrum, which is $-3.18 \pm$

0.21 for GLEs, compared to -4.34 ± 0.19 for non-GLEs. Giacalone (2005) has shown that shock acceleration at quasi-perpendicular shocks can proceed much more rapidly and provide harder spectral indices than acceleration at parallel shocks (see also Zank et al. 2006). In addition, Tylka et al. (2005, 2006) and Tylka and Lee (2006) have suggested that acceleration at quasi-perpendicular shocks can explain the enrichment of Fe and other heavy species (discussed below) if quasi-perpendicular shocks have a higher injection threshold, such that they accelerate mainly suprathermal ions.

Composition Signatures Many GLEs exhibit properties generally associated with "flare material" as observed in impulsive (^{3}He-rich) SEP events (e.g., Mason et al. 1994; Reames et al. 1994; Mason et al. 2004) including enrichments in Fe/O, Ne/O, ^{22}Ne/^{20}Ne, and highly-ionized charge states of Fe. Following work by Dietrich and Lopate (1999), Tylka et al. (2005) reported that 23 of 25 GLEs during solar cycles 21 and 22 had 46–80 MeV/nuc Fe/O ratios that were enriched by a factor of $\geq$2 with respect to the average SEP abundances of Reames (1995), in which Fe/O = 0.134. Their survey was based on IMP-7&8 data from the University of Chicago instrument. During solar cycle 23 we find a considerably lower incidence of Fe-rich GLE events, with 9 of the 16 GLEs (56 ± 12 %) in Table 2 having an Fe/O enrichment of $\geq$2.0 in the 45 to 80 MeV/nuc interval (see also Fig. 8). By comparison, the sample of 30 non-GLE events had an Fe/O enrichment of $\geq$2.0 in 33 ± 9 % of the cases. It is possible that some GLE events became more enriched in Fe at energies >80 MeV/nucleon; in 9 of the 16 cycle-23 GLE events Fe/O was increasing with energy (see Table 2 and examples in Tylka et al. 2005). However, the fraction of GLE events that were Fe-rich during solar cycle 23 is apparently considerably less than was found by Dietrich and Tylka (2003) for solar cycles 21 & 22.

Among the possibilities suggested to explain flare signatures in SEP events associated with both large flares and fast CMEs are the following: (1) shock acceleration of remnant suprathermal ions in the interplanetary medium left from previous impulsive SEP events (Mason et al. 1999; Tylka et al. 2005; Mewaldt et al. 2006; Tylka and Lee 2006); (2) mixed contributions from escaping flare-accelerated particles and CME shock-accelerated particles (Cane et al. 2003, 2006); (3) shock acceleration of a mixture of solar wind and escaping flare particles (Li and Zank 2005); and (4) acceleration of a mixture of suprathermals and CME ejecta (Mewaldt et al. 2007). Li et al. (2012; see also Li and Mewaldt 2009) discuss a model where CME and flare-accelerated material may be shock-accelerated when two closely spaced CMEs interact. The data presented here do not distinguish clearly between these various possibilities.

Ionic Charge States For five of the GLE events (and two non-GLE events) the mean ionic charge state of Fe ($\langle Q_{\rm Fe} \rangle$) is found to be $\sim +20$, corresponding to an equilibrium temperature of $\sim$10 MK (Mazzotta et al. 1998). The highly-ionized >20 MeV/nuc ions in these events could also be the result of electron stripping during the acceleration and/or transport process (e.g., Barghouty and Mewaldt 1999, 2000; Kovaltsov et al. 2001; Lytova and Kocharov 2005). Kovaltsov et al. (2001) find that to strip Fe from a typical solar-wind charge state ($\langle Q_{\rm Fe} \rangle \approx 10$) to $\langle Q_{\rm Fe} \rangle \geq 18$ during acceleration from $\sim$0.1 to 30 MeV/nuc requires that the product of the density (n) and acceleration time (τ) be $n\tau \geq 7.5 \times 10^9$ s/cm^3 (see also Kocharov 2006). Electron stripping (along with adiabatic energy loss) has been shown to play an important role in explaining the energy-dependent charge states observed in small impulsive ^{3}He-rich events (Klecker et al. 2006, 2007), but these events originate low in the corona. It is not obvious that ions accelerated at a CME-driven shock in the high corona will pass through sufficient material.

Table 3 Estimated acceleration start point to traverse $n\tau = 7.5 \times 10^9$ s/cm^3 and strip Fe ions to $Q \geq +18$

GLE event	Q_{Fe}[1]	CME space speed (km/s)[2]	Estimated latitude difference from CS	Required acceleration height (Rs) for $Q_{Fe} \geq 18$	Type-II formation height (Rs)[2]
11/6/97	19.6 ± 2.4	1726	~31°	≤1.24	1.31
5/2/98	19.3 ± 3.0	1332	~8°	≤1.55	1.41
5/6/98	21.5 ± 2.5	1208	~12°	≤1.53	1.29
4/15/01	22.1 ± 2.9	1203	~6°	≤1.60	1.52
12/26/01	20.7 ± 2.6	1779	~0°	≤1.49	1.48
7/14/00	13.7 ± 1.7	1741	~7°	≤1.47	1.39
11/4/01	11.9 ± 1.3	1846	~35°	≤1.20	1.43
10/28/03	14.5 ± 2.0	2754	~25°	≤1.20	1.27
1/20/05	11.7 ± 1.8	3675	~0°	≤1.27	1.81
12/13/06	16.0 ± 2.0	2164	~24°	≤1.25	1.58

[1]Labrador et al. (2005)

[2]Table 1 of Gopalswamy et al. (2012)

We attempt to check whether this is reasonable using the observed properties of the associated CMEs and Type-II radio bursts for these events (Gopalswamy et al. 2012). We consider a strong shock (density jump of ~4), and assume that Fe ions are trapped at the nose of the shock, spending equal time on either side of the density jump. In the following we use CME space speeds rather than the sky-plane speeds observed by a coronagraph. The CME space speeds (see Table 3) were estimated by Gopalswamy et al. (2012) by applying a projection correction using a cone model (Xie et al. 2004). Thus the accelerated Fe ions are assumed to move outward at the CME space speed until they are released higher in the corona (we assumed 20 Rs), where the density has dropped by a factor of >1000 (10 Rs gives very similar results).

Under this assumption the $n\tau$ product can be estimated using the coronal density profile in the model of Guhathakurta et al. (1996; here-in-after GHM), including their model of the current sheet (CS) density. Note that in this picture the stripping probability is inversely proportional to the CME space speed. Five of the 16 GLE events had Fe charge-state estimates that were highly ionized at >25 MeV/nuc ($\langle Q_{Fe} \rangle \approx 20$; Labrador et al. 2005, Cohen et al. 1999a, 1999b) and they are listed first in Table 3. It is interesting that the average CME space speed for these events was 1450 km/s, while the average CME space speed for the five events with $\langle Q_{Fe} \rangle \leq 16$ was 2436 km/s.

For all 10 events we have estimated the height in the corona where the acceleration must start to achieve $n\tau = 7.5 \times 10^9$ s/cm^3. The flare location and synoptic magnetic field maps from Wilcox observatory (http://wso.stanford.edu/) were used to estimate the distance (in degrees) from the current sheet (CMEs originating near the current sheet encounter a greater overlying coronal density). Then, Eq. (10) of GHM was used to calculate radial and latitudinal density profiles for each event. Using these density profiles the $n\tau$ product (at the nose of the CME) was calculated as a function of the height where acceleration started, integrating along a single pathlength projected radially from the flare site. For the five highly-ionized events we find that acceleration must start between ~1.24 and ~1.60 Rs. For the other five events the acceleration would need to start between ~1.20 to ~1.47 Rs to achieve $n\tau = 7.5 \times 10^9$ s/cm^3.

In Table 3 and Fig. 12 we compare the location required to meet $n\tau \approx 7.5 \times 10^9$ s/cm^3 to estimates Gopalswamy et al. (2012) of the height of the CME at the onset of the Type-II radio burst (indicating that a shock has formed). These estimates take into account CME

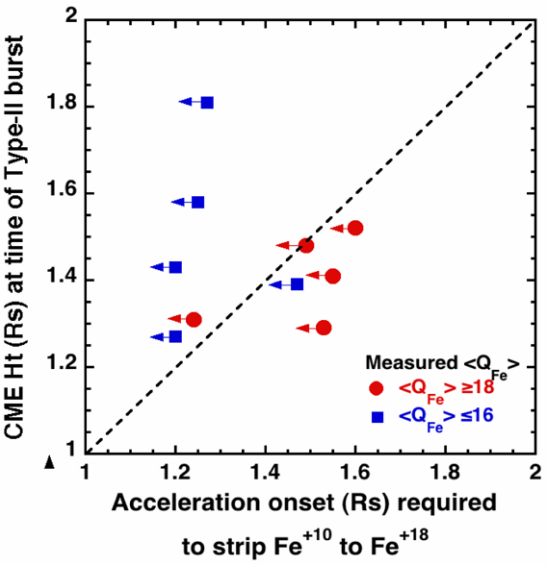

Fig. 12 The CME heliocentric height at the onset of the Type-II burst (Gopalswamy et al. 2012) is plotted versus an estimate of the height where shock acceleration must occur to achieve a density-time product of $n\tau = 7.5 \times 10^9$ s/cm^3 (see text for details). The ten GLE events for which there are Fe charge-state measurements or estimates above 10 MeV/nuc are divided into two groups, those with $\langle Q_{\rm Fe}\rangle \geq 18$ and those with $\langle Q_{\rm Fe}\rangle \leq 16$. For events to the right of the *dashed line* $\langle Q_{\rm Fe}\rangle \geq 18$ is expected, for events to the left it is not. For eight of the ten events the measurements fit the expected pattern

acceleration in the low-corona (see their paper for a discussion of the uncertainties in these estimates). For four of the five highly-ionized events (all but 6 November 1997) the CME height at the onset of the Type-II burst was below the required height for starting acceleration, indicating that stripping to $\langle Q_{\rm Fe}\rangle \geq 18$ was possible. For four of the last five events in Table 3 (those with $\langle Q_{\rm Fe}\rangle \leq 16$) the CME height at the onset of the Type-II burst was above the required height for starting acceleration (the exception was 14 July 2000), indicating that stripping to $\langle Q_{\rm Fe}\rangle \geq 18$ was not likely if the accelerated ions had typical solar-wind charge states when injected. Of course, this is a highly simplified picture—as CMEs expand they encounter a broad range of densities. In particular, we can expect that $n\tau$ will be greater for acceleration at the flanks of the shock than at the nose since the shock speed is likely to be lower, and the initial shock direction is non-radial, allowing accelerated ions to sample higher densities for a longer time.

This comparison provides support for the idea that stripping of SEP ions during acceleration is a cause of (or at least contributes to) highly-ionized charge-states in some large SEP events. The scenario discussed here predicts that events with slower CMEs will have higher $\langle Q_{\rm Fe}\rangle$ values, as is observed (the five events with $\langle Q_{\rm Fe}\rangle \approx 20$ were associated with CMEs that were slower by an average of ∼1000 km/s) and it predicts higher charge states for events where acceleration starts lower in the corona (the estimated CME height at the time of Type-II bursts averaged 1.40 Rs for the five high charge-state events and 1.50 Rs for the remaining five events).

An important ingredient in this comparison is improved estimates of the CME location at the onset of the Type-II radio burst. In an earlier paper Gopalswamy et al. (2009) compared high-cadence STEREO images of CMEs starting at ∼1.4 Rs with Type-II bursts observed by STEREO and Wind and found that during the declining phase of solar cycle 23 CME-driven shocks typically started at ∼1.5 Rs, which is near the altitude where the coronal Alfven speed reaches a minimum value (∼1.4 Rs). This compares to an average height of ∼2.2 Rs determined from CMEs observed by the SOHO/LASCO C2 coronagraph, for which coronal images start at 2.5 Rs (Gopalswamy et al. 2005; see also Reames 2009).

Most of the reduction in the inferred altitudes based on STEREO data is due to accounting for CME acceleration in the low corona (observed directly by STEREO), rather than extrapolating to lower heights with a constant speed, as in Gopalswamy et al. (2005, 2010). It is also interesting that Cliver et al. (2001, 2005), based on LASCO/C1 data down to 1.1 Rs, found that the Type-II burst in the 6 November 1997 event began with the CME $\leq$1.4 Rs [while Gopalswamy (2010) found 2.87 Rs using LASCO/C2 data, now revised to 1.31 Rs in Gopalswamy et al. (2012) by accounting for CME acceleration].

At least four of the five highly-ionized events in Table 3 had preceding CMEs (Gopalswamy et al. 2004, 2010; Ding et al. 2011), which may have produced elevated plasma densities in the path of the second CME and could also have left higher densities of suprathermal seed particles and enhanced turbulence levels (Li et al. 2012).

Mewaldt et al. (2006) concluded that a major source of seed particles for CME shocks is remnant low-energy SEPs from preceding large SEP events, which they found are also Fe-rich, on average (see their Fig. 11). If low-energy Fe ions from a previous CME-shock event remain in the low corona for several hours they will be ionized further, and approach an equilibrium charge of +16 at ~0.2–0.5 MeV/nuc and +20 or more at >1 MeV/nuc (see Fig. 2 in Kovaltsov et al. 2001). At the same time these ions will cool due to adiabatic and dE/dx energy losses, which can produce a highly-ionized seed-population ready for acceleration by the next CME-driven shock. It is interesting that the cooled ions tend to retain their high charge states because recombination rates are ~10 times longer than stripping rates [see Fig. 8 in Kocharov et al. (2000) and Fig. 7 in Kocharov et al. (2001)]. These energetic ions can jump-start the injection process and, because of Q/A-dependent trapping at the shock (Cohen et al. 2005; Mewaldt et al. 2005a, 2005b; Li et al. 2009) will be accelerated to somewhat higher energies than ions with solar-wind-like charge states. This stripping/cooling mechanism can produce abundant seed particles with $\langle Q_{\mathrm{Fe}} \rangle \approx 16$–$20$ and more, without the need for remnant highly-ionized Fe from (generally small) ^{3}He-rich flares. Modeling is needed to evaluate the density of seed particles produced in this way (see also Kocharov 2006).

It is important to consider whether there will be a sufficient density of accelerated ions downstream of the first shock to be accelerated by the second shock. Perhaps the best evidence for this comes from Helios data analyzed by Reames et al. (1997), who measured SEP spectra and intensities following 29 shocks observed by Helios 1 from 0.33 to 1 AU during 1979 to 1982. They found that following shock passage "invariant spectra" are observed with intensities that decay gradually with e-folding times of 6–18 hours for periods of ~3 days. These invariant spectra remain well above quiet-time intensity levels for days, and will provide seed particles for a subsequent CME-driven shock that occurs within the next 24 hours or so. This is likely to be one factor that contributes to the observation by Gopalswamy et al. (2004) that SEP events preceded by a CME from the same active region <24 hours earlier are, on average, significantly more intense that those with no preceding CME.

Of course, there are other suggested explanations for observations of highly-ionized charge states in large SEP events, including a seed particle population composed largely of remnant material from small ^{3}He-rich flares (Mason et al. 1999; Tylka et al. 2005; Tylka and Lee 2006), CME material from previous events (Mewaldt et al. 2007; Li et al. 2012), or mixtures of flare and shock-accelerated particles from the same eruption (Cane et al. 2003, 2006). While these models do not make specific predictions about the degree of ionization in individual events, they do predict a correlation between highly-ionized charge states, enrichments in heavy elements, and elevated ^{3}He/^{4}He ratios.

We can also ask how long suprathermal ions from small, ^{3}He-rich flares remain near the Sun? Simulations by Giacalone et al. (2000) show that following an impulsive flare there is

still a significant fraction of the low-energy ions that remain close to the Sun, and of course, in many cases these small ^{3}He-rich events recur several times a day (Wang et al. 2006). These remnant ions will also undergo further ionization and energy loss.

We conclude that electron stripping during acceleration and transport provides a viable mechanism for producing highly-ionized heavy ions in SEP events. However it does not preclude contributions from the other proposed mechanisms. For example, the fact that many CME-shock accelerated SEP events have ^{3}He/^{4}He ratios ∼100 to ∼1000 times greater than in the solar wind provides strong evidence that remnant material from impulsive ^{3}He-rich events provides seed material for later CME-driven shocks (e.g., Mason et al. 1999; Desai et al. 2006). However, in small impulsive events the Fe/^{3}He ratio is ∼0.1, while in the large SEP events with both ^{3}He and Fe enrichments Fe/^{3}He ∼1 (Mewaldt et al. 2006). So it would appear that in the largest SEP events an additional source of Fe seed particles is needed (other than remnant ^{3}He-rich flare material), and since most GLE events occur in a sequence of several SEP events, remnant energetic ions from earlier CME-driven-shocks are an inevitable source of seed particles for subsequent events. The upcoming Solar Probe Plus and Solar Orbiter missions will be able to test these ideas with measurements close to the Sun.

Energetics of GLE Events The fact that GLE events have harder spectra on average allows smaller SEP events to accelerate many more protons >0.5 GeV than in typical SEP events that derive approximately the same amount of energy from the accelerator. This is illustrated by the two hypothetical spectra in Fig. 13. Although both spectra have identical proton fluences >500 MeV (the energy range responsible for the GLE event), for the (dashed blue) event with the harder spectrum above the break at 20 MeV (labeled B1 in Fig. 13) the measured SEP kinetic energy (in MeV/cm^2) would be >200 times smaller.

In an effort to identify the variables that are key to producing a GLE event with the least amount of energy, we make use of the "GLE percentage" (GLE % for short), defined as the maximum value of the ratio of two count rates: (1) the peak neutron-monitor count rate due to SEPs and (2) the underlying neutron-monitor count rate due to galactic cosmic rays (see, e.g., Lopate 2006; Gopalswamy et al. 2010, 2012). We assume that the GLE % is a function

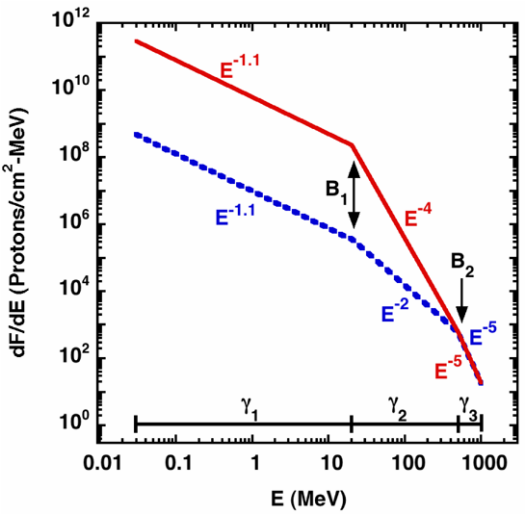

Fig. 13 Proton energy spectra for two hypothetical GLEs with identical fluences >500 MeV, but very different spectra at lower energy. The assumed spectral indices (γ_1, γ_2 and γ_3) are shown in 3 energy intervals (0.03–20 MeV; 20–500 MeV; and 500–1000 MeV). Also indicated are the locations of the spectral breaks at 20 MeV and 500 MeV. The estimated kinetic energy content (in ergs/cm^2) for the event shown in red is >200 times more than that for the event shown in *blue*

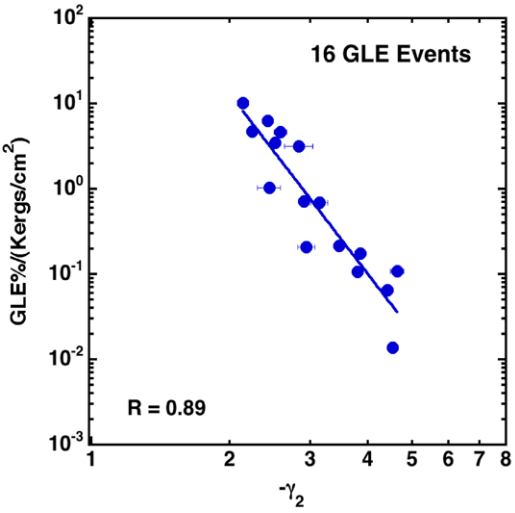

Fig. 14 The GLE % [defined as the ratio of the peak GLE intensity to the GCR intensity (from Gopalswamy et al. 2010, 2012) is divided by the 40 keV–400 MeV energy deposit ($\langle$E/cm$^2\rangle$ in Kerg/cm^2; see text)] and plotted versus the absolute value of the spectral index above the first spectral break (γ_2 in Table 1). The least-square fit to a power-law has a correlation coefficient of $R = 0.89$. One way to interpret this relation is to write it as GLE % $= 1700\langle$E/cm$^2\rangle|\gamma_2|^{-7.0}$, suggesting that the SEP excess above the GCR background is a function of the near-Earth SEP energy content times a strong function of the spectral index

of the near-Earth SEP energy content (integrated over energy and time) and also the spectral index and possibly the flare longitude.

In Fig. 14 we see that the GLE % divided by the SEP energy content is strongly correlated with the spectral index above the break (γ_2 in Table 1). One way to interpret this correlation is to write it as GLE % $= 1700\langle$E/cm$^2\rangle|\gamma_2|^{-7.0}$, where $\langle$E/cm$^2\rangle$ is the MeV/cm^2 integrated over the fluence from 40 keV to 400 MeV (using the spectral fits in Table 1). In other words, SEP events with hard spectra in the energy range covered by γ_2 are much more energy efficient—they can produce a GLE event using only a small fraction of the energy in accelerated particles that is measured in events that have soft spectra. The connection longitude is another variable that might also be expected to matter, but the correlation with flare-longitude substituted for γ_2 (not shown) has a correlation coefficient of only $R = 0.37$. For comparison, the correlation coefficient of the low-energy spectral index (γ_1) is slightly negative with $R = 0.18$.

The importance of γ_2 is also illustrated by comparing the GLE %/$\langle$E/cm$^2\rangle$ values for the 13 December 2006 event at W23° ($\gamma_2 = -2.42$; see Fig. 6) with either the 4 November 2001 event at W18° (Fig. 4) or the 17 January 2005 event at W25° (Fig. 6). Both of the latter events (at similar longitudes) have $\gamma_2 \leq -4.5$ and their GLE %/$\langle$E/cm$^2\rangle$ values in Fig. 14 are ∼80 to ∼400 times less than that of the 13 December 2006 event. We conclude that the most energy-efficient way to produce GLE events is with hard spectra in the energy range covered by γ_2.

Mewaldt et al. (2005a, 2008b) found that large SEP events often extract ∼10 % of the kinetic energy from the CME (estimated in the rest frame of the solar wind). The most energetic SEP events of solar cycle 23 include the July 14, 2000 (Bastille Day) event, the November 4, 2001 event, and the October 28, 2003 event. The associated CMEs had kinetic energies ranging from ∼1.2 to $\sim 9 \times 10^{32}$ ergs. Only ∼0.5 % of all 4133 CMEs (or ∼20

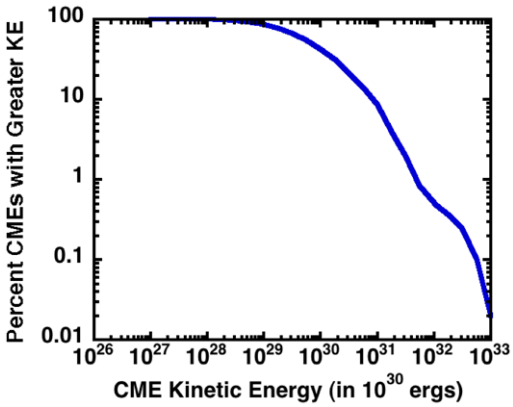

Fig. 15 Integral distribution of CME kinetic energies for 4133 CMEs measured by the SOHO/LASCO instrument from 1996 to 2003 (adapted from Gopalswamy 2006)

CMEs) measured by SOHO/LASCO from 1996 to 2003 had kinetic energies $> 1.2 \times 10^{32}$ ergs (see Fig. 15 and Gopalswamy 2006), meaning that a significant fraction of these produced GLEs from 1997 to 2003. (Indeed, of the 11 GLEs from 1997 to 2003 for which there are kinetic energy measurements, 7 had CME kinetic energies $\geq 1.2 \times 10^{32}$ ergs; see Gopalswamy et al. 2004, 2005.)

On the other hand, the May 2 and May 6, 1998 CMEs had estimated kinetic energies of $\sim 1.0 \times 10^{31}$ and $\sim 6 \times 10^{31}$ ergs, respectively, and relatively hard spectra ($\gamma_2 = -2.83$ and -2.58, respectively). Figure 15 indicates that ~8 % of all CMEs (or ~330 CMEs) had kinetic energies $\geq 1 \times 10^{31}$ ergs. In other words, there were >300 CMEs that were energetically capable of producing a GLE event provided they encountered the right conditions to produce very hard spectra ($\gamma_2 \geq -2.8$) up to energies of ~500 MeV. Evidently these conditions are not that common; the additional ~300 CMEs resulted in only 2 additional GLEs.

5 Summary

Proton fluence spectra for the sixteen GLE events of solar cycle 23 have been measured from ~0.1 to ~500–700 MeV with a combination of instruments from ACE, GOES, SAMPEX, and STEREO. After considering a variety of spectral forms it was found that all 16 events were best fit by the double power-law shape of Band et al. (1993). The average spectral break (defined by the intersection of the two power laws) was ~18 MeV. While there are suggested conditions for producing double-power-law spectra, additional theoretical and modeling work is needed to understand how such spectra originate.

When compared to a sample of more typical large non-GLE events we find that the GLE events have significantly harder energy spectra above the spectral break energy, with a mean slope of -3.18 above the break, compared to a mean of -4.34 for a sample of 22 non-GLE events. The harder spectra observed in GLE events are related to the energetics of SEP events. We find that SEP events with very hard spectra from ~20 to ~400 MeV require much less energy content to stand out above the GCR background. Thus, a larger population of CMEs has the potential to produce GLEs. Based on limited statistics it appears that a GLE resulted from ~30 % of the observed CMEs that had kinetic energies of $\geq 10^{32}$ ergs during 1996–2003.

This study also reported several aspects of the composition of GLE events. On average, GLE events have larger Fe/O ratios than a sample of non-GLE events, and also exhibit

other compositional signatures associated with small, ^{3}He-rich events, including elevated Ne/O and ^{22}Ne/^{20}Ne ratios, and highly-ionized charge-states of heavy elements such as Fe. However, we find a significantly lower incidence of Fe enrichments in the 45 to 80 MeV/nuc interval than did the study of Tylka et al. (2005), with Fe/O enrichments of $\geq$2.0 in 9 of 16 cycle-23 events, compared to their finding of Fe enrichments in 23 of 25 GLE events from cycles 21 and 22. These abundance features generally support a picture in which GLE events are accelerated mainly by CME-driven shocks, with shock geometry playing a key role, and with seed particles derived mainly from remnant suprathermal ions from small ^{3}He-rich flares and from larger shock-accelerated events (although contributions from other sources are also possible).

A possible cause for elevated charge states of Fe (e.g., $\langle Q_{\mathrm{Fe}} \rangle \approx 20$) in GLE and other large SEP events is electron stripping, provided that shock-acceleration starts sufficiently low in the corona. Using a coronal density model, including current-sheet effects, we find that it is possible to meet the required density acceleration-time product if acceleration starts by $\sim$1.3 to 1.6 Rs, consistent with recent comparisons of Type-II radio-burst timing with CME height-versus-time profiles that view CMEs down to 1.4 Rs and below and/or take into account the CME acceleration profile in the low corona. In addition, the fact that almost all GLE events had preceding CMEs suggests that remnant shock-accelerated particles left behind in the low corona can undergo stripping and energy-loss to produce a highly-ionized seed population for the next fast CME. Detailed modeling is needed to evaluate the contributions from these processes.

Most of these ideas can be tested with measurements near the Sun by the upcoming Solar Orbiter and Solar Probe Plus missions. In the meantime, multi-spacecraft studies with separated spacecraft (STEREO, ACE, SOHO, Wind and MESSENGER) should gain new insight into the mechanisms that shape and accelerate the GLE events of cycle 24.

Acknowledgements This work was supported by NASA at Caltech under grants NNX8AI11G and NNX06AC21G, and under subcontract SA2715-26309 from UC Berkeley under NASA contract NAS5-03131. We appreciate the availability of GOES data at the NOAA website, SOHO CME data at the Catholic University website, and thank Allan Tylka for advice on using HEPAD data. We are grateful for helpful suggestions from both reviewers. Finally, we thank Nat Gopalswamy and Nariaki Nitta for helpful discussions, for organizing the two LWS workshops on GLEs, and for serving as editors for this volume.

References

R. Abbasi et al., Astrophys. J. Lett. **689**, L65 (2008)
D.N. Baker et al., IEEE Trans. Geosci. Remote Sens. **31**, 531 (1993)
D.N. Baker, L.A. Braby, S. Curtis, J.R. Jokipii, W.S. Lewis, J. Miller, W. Schimmerling, H.J. Singer, L. Strachan, L.W. Townsend, R.E. Turner, T.H. Zurbuchen, *Space Radiation Hazard and the Vision for Space Exploration* (Academies Press, Washington, 2006)
D. Band et al., Astrophys. J. **413**, 281 (1993)
A.F. Barghouty, R.A. Mewaldt, Astrophys. J. Lett. **520**, L127 (1999)
A.F. Barghouty, R.A. Mewaldt, in *Acceleration and Transport of Energetic Particles Observed in the Heliosphere*. AIP. Conf. Proc., vol. 528 (2000), p. 71
H.V. Cane, T.T. von Rosenvinge, C.M.S. Cohen, R.A. Mewaldt, Geophys. Res. Lett. **30** (2003). doi:10.1029/2002GL016580
H.V. Cane, R.A. Mewaldt, C.M.S. Cohen, T.T. von Rosenvinge, J. Geophys. Res. **111**, AOS690 (2006). doi:10.1029/2005JA011071
E.W. Cliver, A. Falcone, J. Ryan, H. Aurass, L.C. Gentile, M.-B. Kallenrode, A.-G. Ling, M.J. Reiner, O.C. St. Cyr, M. Yoshimori, *27th Internat. Cosmic Ray Conf.*, vol. 8 (2001), p. 3276
E.W. Cliver, N.V. Nitta, B.J. Thompson, J. Zhang, Sol. Phys. **225**, 105 (2005)
C.M.S. Cohen et al., Geophys. Res. Lett. **26**, 149 (1999a)
C.M.S. Cohen et al., Geophys. Res. Lett. **26**, 2697 (1999b)

C.M.S. Cohen, R.A. Mewaldt, A.C. Cummings, R.A. Leske, E.C. Stone, T.T. von Rosenvinge, M.E. Wiedenbeck, Adv. Space Res. **32**, 2649 (2003)
C.M.S. Cohen, E.C. Stone, R.A. Mewaldt, R.A. Leske, A.C. Cummings, G.M. Mason et al., J. Geophys. Res. **110** (2005). doi:10.1029/2004JA011004
W.R. Cook et al., IEEE Trans. Geosci. Remote Sens. **31**, 565 (1993a)
W.R. Cook et al., IEEE Trans. Geosci. Remote Sens. **31**, 557 (1993b)
H. Debrunner, E. Flueckiger, J.A. Lockwood, R.E. McGuire, J. Geophys. Res. **89**, 769 (1984)
H. Debrunner, E. Flueckiger, H. Graedel, J.A. Lockwood, R.E. McGuire, J. Geophys. Res. **93**, 7206 (1988)
M.I. Desai, G.M. Mason, R.E. Gold, S.M. Krimigis, C.M.S. Cohen, R.A. Mewaldt, J.E. Mazur, J.R. Dwyer, Astrophys. J. **649**, 470–489 (2006)
W. Dietrich, C. Lopate, in *Proc. 26th Int. Cosmic Ray Conf.*, Salt Lake City, vol. 6 (1999), p. 71
W.F. Dietrich, A.J. Tylka, in *28th Internat. Cosmic Ray Conf.*, Tskuba, Japan, vol. 6 (2003), p. 3291
L. Ding, Y. Jiang, L. Zhao, G. Li, The twin-CME scenario and large solar energetic particle events in solar cycle 23. J. Geophys. Res. (2011, submitted)
D.C. Ellison, R. Ramaty, Astrophys. J. **298**, 400 (1985)
A. Falcone et al., Astrophys. J. **588**, 557 (2003)
S.E. Forbush, Phys. Rev. **70**, 771 (1946)
M.S. Forman, R. Ramaty, E.G. Zweibel, in *The Physics of the Sun*, ed. by P.A. Sturrock, T.E. Holzer, D. Mihalas, R.K. Ulrich, vol. II (Reidel, Dordrecht, 1986), p. 249
J. Giacalone, Astrophys. J. **624**, 765 (2005)
J. Giacalone, J.R. Jokipii, J.E. Mazur, Astrophys. J. **532**, L75 (2000)
R.E. Gold et al., Space Sci. Rev. **86**, 541 (1998)
N. Gopalswamy, J. Astrophys. Astron. **27**, 243 (2006)
N. Gopalswamy, S. Yashiro, S. Krucker, G. Stenborg, R.A. Howard, J. Geophys. Res. **109**, A12105 (2004). doi:10.1029/2004JA010602
N. Gopalswamy, S. Yashiro, Y. Liu, G. Mihalek, A. Vourlidas, M.L. Kaiser, R.A. Howard, J. Geophys. Res. **110**, A09S15 (2005). doi:10.1029/2004JA010958
N. Gopalswamy et al., Sol. Phys. (2009). doi:10.1007/s11207-009-9382-1
N. Gopalswamy, H. Xie, S. Yashiro, I. Usoskin, Indian J. Radio & Space Phys. **39**, 240 (2010)
N. Gopalswamy, H. Xie, S. Yashiro, S. Akiyama, P. Makela, I.G. Usoskin, Space Sci. Rev. (2012, in press). doi:10.1007/s11214-012-9890-4
M. Guhathakurta, T.E. Holzer, R.M. MacQueen, Astrophys. J. **458**, 817 (1996)
B.E. Klecker, E. Moebius, M.A. Popecki, L.M. Kistler, H. Kucharek, M. Hilchenbach, Adv. Space Res. **38**(3), 493 (2006)
B.E. Klecker, E. Moebius, M.A. Popecki, Space Sci. Rev. **130**, 273 (2007)
L. Kocharov, in *Solar Eruptions & Energetic Particles*, ed. by N. Gopalswamy, R.A. Mewaldt, J. Torsti. AGU Monograph Series (2006), p. 137
L. Kocharov, G.A. Kovaltsov, J. Torsti, V.M. Ostryakov, Astron. Astrophys. **357**, 716 (2000)
L. Kocharov, G.A. Kovaltsov, J. Torsti, Astrophys. J. **556**, 919 (2001)
G.A. Kovaltsov, A.F. Barghouty, L. Kocharov, V.M. Ostryakov, J. Torsti, Astron. Astrophys. **375**, 1075 (2001)
A.W. Labrador, R.A. Leske, R.A. Mewaldt, E.C. Stone, T.T. von Rosenvinge, in *Proc. 29th Internat. Cosmic Ray Conf. (Tskuba)*, vol. 1 (2005), p. 99
R.A. Leske, J.R. Cummings, R.A. Mewaldt, E.C. Stone, T.T. von Rosenvinge, Astrophys. J. Lett. **452**, L149 (1995)
R.A. Leske, R.A. Mewaldt, C.M.S. Cohen, A.C. Cummings, E.C. Stone, M.E. Wiedenbeck, T.T. von Rosenvinge, Space Sci. Rev. **130**, 195 (2007)
G. Li, G.P. Zank, Geophys. Res. Lett. **32**, L02101 (2005). doi:10.1029/2004GL021250
G. Li, R.A. Mewaldt, 31st Internat. Cosmic Ray Conf., Paper 1362 (2009)
G. Li, G.P. Zank, W.K.M. Rice, J. Geophys. Res. **108** (2003). doi:10.1029/2002JA009666
G. Li, Q. Hu, G.P. Zank, in *The Physics of Collisionless Shocks*, ed. by G. Li, G.P. Zank, C.T. Russell. AIP CP, vol. 781 (AIP, New York, 2005), p. 223
G. Li, G.P. Zank, O. Verkhoglyadova, R.A. Mewaldt, C.M.S. Cohen, G.M. Mason, M.I. Desai, Astrophys. J. **702**, 998 (2009)
G. Li, R. Moore, R.A. Mewaldt, L. Zhao, A.W. Labrador, Space Sci. Rev. (2012, this issue). doi:10.1007/s11214-011-9823-7
J.A. Lockwood, W.R. Webber, L. Hsieh, J. Geophys. Res. **79**, 4149 (1974). doi:10.1029/JA079i028p04149
C. Lopate, in *Solar Eruptions and Energetic Particles*, ed. by N. Gopalswamy, R.A. Mewaldt, J. Torsti. AGU Monograph Series (2006), p. 283
M. Lytova, L. Kocharov, Astrophys. J. Lett. **620**, L55 (2005)
G.M. Mason, J.E. Mazur, D.C. Hamilton, Astrophys. J. **425**, 843 (1994)
G.M. Mason et al., Space Sci. Rev. **86**, 409 (1998)

G.M. Mason et al., Astrophys. J. Lett. **525**, L133 (1999)
G.M. Mason, J.E. Mazur, J.R. Dwyer, J.R. Jokipii, R.E. Gold, S.M. Krimigis, Astrophys. J. **606**, 555 (2004)
J.E. Mazur, G.M. Mason, B. Klecker, R.E. McGuire, Astrophys. J. **401**, 398 (1992)
P. Mazzotta, G. Mazzitelli, S. Colafrancesco, N. Vittorio, Astron. Astrophys. Suppl. Ser. **133**, 403 (1998)
R.E. McGuire, T.T. von Rosenvinge, Adv. Space Res. **4**(2–3), 117 (1984)
A. Meshik et al., Science **318**, 433 (2007)
R.A. Mewaldt et al., J. Geophys Res. **110** (2005a). doi:10.1029/2005JA011038
R.A. Mewaldt et al., in *The Physics of Collisionless Shocks*, ed. by G. Li, G.P. Zank, C.T. Russell. AIP Conf. Proc., vol. 781 (AIP, New York, 2005b), p. 227
R.A. Mewaldt, C.M.S. Cohen, G.M. Mason, in *Solar Eruptions and Energetic Particles*, ed. by N. Gopalswamy, R.A. Mewaldt, J. Torsti. AGU Monograph Series (2006), p. 115
R.A. Mewaldt et al., Space Sci. Rev. **130**, 207 (2007)
R.A. Mewaldt et al., Space Sci. Rev. **136**, 285 (2008a)
R.A. Mewaldt et al., in *Particle Acceleration and Transport in the Heliosphere and Beyond*, ed. by G. Li, Q. Hu, O. Verhoglyadova, G.P. Zank, R.P. Lin, J. Luhmann. AIP Conference Proc, vol. 1039 (AIP, New York, 2008b), p. 111
T.G. Onsager et al., SPIE Proc. Ser. **2812**, 281 (1996)
R. Ramaty, *Particle Acceleration Mechanisms in Astrophysics—Proceedings of the Workshop* (American Institute of Physics, New York, 1979), p. 135
R. Ramaty, R.J. Murphy, Space Sci. Rev. **45**, 213 (1987)
D.V. Reames, Adv. Space Res. **15**(7), 41 (1995)
D.V. Reames, Astrophys. J. **693**, 812 (2009)
D.V. Reames, S.W. Kahler, C.K. Ng, Astrophys. J. **491**, 414 (1997)
D.V. Reames, J.P. Meyer, T.T. von Rosenvinge, Astrophys. J. Suppl. Ser. **90**, 649 (1994)
D.V. Reames, C.K. Ng, Astrophys. J. **723**, 1286 (2010)
M.A. Shea, D.F. Smart, Space Sci. Rev. (2012, this issue)
D.F. Smart, M.A. Shea, Radiat. Meas. **30**, 327 (1999)
L.S. Sollitt et al., Astrophys. J. **679**, 910 (2008)
E.C. Stone et al., Space Sci. Rev. **86**, 357 (1998)
A.J. Tylka, J. Geophys. Res. **106**, 25333 (2001)
A.J. Tylka, personal communication (2009)
A.J. Tylka, W.F. Dietrich, 31st Internat. Cosmic Ray Conf., Paper 273 (2009)
A.J. Tylka, M.A. Lee, Astrophys. J. **646**, 1319 (2006)
A.J. Tylka, P.R. Boberg, R.E. McGuire, C.K. Ng, D.V. Reames, in *Acceleration and Transport of Energetic Particles Observed in the Heliosphere*. AIP. Conf. Proc, vol. 528 (2000), p. 147
A.J. Tylka, C.M. S Cohen, W.F. Dietrich, M.A. Lee, C.G. Maclennan, R.A. Mewaldt, C.K. Ng, D.V. Reames, Astrophys. J. **625**, 474 (2005)
A.J. Tylka, C.M. S Cohen, W.F. Dietrich, M.A. Lee, C.G. Maclennan, R.A. Mewaldt, C.K. Ng, D.V. Reames, Astrophys. J. Suppl. Ser. **164**, 536 (2006)
R. Vainio, Astron. Astrophys. **406**, 735 (2003)
M.A.I. Van Hollebeke, F.B. McDonald, J.P. Meyer, Astrophys. J. Suppl. Ser. **73**, 285 (1990)
T.T. von Rosenvinge et al., Space Sci. Rev. **136**, 391 (2008)
Y.-M. Wang, M. Pick, G.M. Mason, Astrophys. J. **639**, 495 (2006)
H. Xie, L. Ofman, G. Lawrence, J. Geophys. Res. **109** (2004). doi:10.1029/2003JA010226
G.P. Zank, G. Li, V. Florinski, Q. Hu, D. Lario, C.W. Smith, J. Geophys. Res. **111**, A06108 (2006). doi:10.1029/2005JA011524